Pharmaceutical Sciences and Drug Design
ISSN: 3062-4428
2021, Volume 1, Page No: 119-134

Available online at: www.galaxypub.co/page/journals

Galaxy Publication

Galaxy Publication

Neddylylation Inhibitor MLN4924 Reactivates TRIM58 through LINC01128-Dependent DNMT1 Sequestration in Acute Myeloid Leukemia

Hannah Scott[1]*, Lucas Green[1]

[1]Department of Phytochemistry, Faculty of Health Sciences, Heidelberg University, Heidelberg, Germany.

***E-mail** ✉ hannah.scott.de@outlook.com

Received: 02 August 2021; **Revised:** 28 October 2021; **Accepted:** 03 November 2021

ABSTRACT

This work aimed to clarify how MLN4924 influences acute myeloid leukemia (AML) biology, focusing on its ability to regulate TRIM58 promoter methylation and the downstream molecular events. RT-qPCR and Western blotting were applied to quantify transcript and protein levels, while methylation-sensitive restriction enzyme–qPCR assessed DNA methylation status. RNA sequencing was used to screen for lncRNAs with altered expression. Subcellular fractionation followed by PCR identified transcript localization. Chromatin immunoprecipitation and RNA immunoprecipitation were used to explore protein–DNA and protein–RNA interactions. An in vivo xenograft system was employed to examine tumor behavior, and immunohistochemistry was used to analyze protein expression in tissue samples. TRIM58 expression was reduced in AML and linked to hypermethylation of its promoter region, an effect reversed by MLN4924. Functional assays showed that TRIM58 contributed to MLN4924-triggered apoptotic signaling by suppressing AKT activation. MLN4924 elevated levels of the tumor-inhibitory lncRNA LINC01128, whose forced expression reproduced the TRIM58-associated antiproliferative and pro-apoptotic actions, including modulation of BAX/BCL-2. LINC01128, predominantly nuclear, interacted with DNMT1 and helped drive demethylation of the TRIM58 promoter, defining a new regulatory mechanism. Knockdown of TRIM58 weakened the impact of MLN4924 on AKT phosphorylation and reduced the subsequent apoptotic response. These findings indicate that MLN4924 enhances LINC01128 expression, enabling it to sequester DNMT1 and prevent TRIM58 promoter methylation, ultimately inhibiting AML progression.

Keywords: DNA methylation, DNMT1, lncRNA LINC01128, Proximal promoter

How to Cite This Article: Scott H, Green L. Neddylylation Inhibitor MLN4924 Reactivates TRIM58 through LINC01128-Dependent DNMT1 Sequestration in Acute Myeloid Leukemia. Pharm Sci Drug Des. 2021;1:119-34. https://doi.org/10.51847/rR232vnf8j

Introduction

Acute myeloid leukemia (AML) continues to pose major therapeutic difficulties due to limited effective therapies [1]. Epigenetic manipulation has become increasingly relevant, with hypomethylating drugs such as azacitidine showing clinical benefit [2]. MLN4924, the prototype inhibitor of the NEDD8-activating enzyme (NAE), blocks cullin neddylation, shuts down Cullin-RING ligase (CRL) activity, and promotes accumulation of CRL substrates, resulting in selective cytotoxicity toward malignant cells [3–5]. Multiple clinical trials have demonstrated its safety and its cooperative effects with azacitidine in AML [6–12]. However, the epigenetic mechanisms associated with its activity remain insufficiently explained.

AML frequently exhibits silencing of tumor-suppressive genes through aberrant promoter methylation [13]. For example, DNMT-mediated hypermethylation of SOCS3 accelerates leukemogenesis and serves as a clinical indicator [14]. Likewise, repression of BCL7A through promoter methylation reduces differentiation and enhances nodal infiltration, correlating with inferior outcomes [15, 16]. SCIN promoter methylation has also been linked to patient prognosis [17]. Collectively, these observations underscore DNA methylation as a central driver influencing AML evolution and therapy responses.

Long non-coding RNAs (lncRNAs) are integral components of epigenetic control. Acting as structural and regulatory hubs, they can influence DNA methylation directly or indirectly and contribute to malignant transformation [18–20]. Previous work from our group showed that MLN4924 reshapes methylation profiles in AML cells and specifically induces demethylation of the TRIM58 promoter [21]. TRIM58 functions as a tumor-suppressive gene in several solid malignancies and is frequently silenced through promoter hypermethylation [22–24]. We therefore proposed that TRIM58 is similarly repressed by methylation in AML and that an lncRNA acts as the intermediary linking MLN4924 activity to TRIM58 reactivation. Clarifying this lncRNA-dependent pathway provides insight into the epigenetic processes underlying MLN4924's anti-AML effects.

Materials and Methods

Study subjects

Peripheral blood from 17 patients diagnosed with AML at the Department of Hematology, First Affiliated Hospital of Lanzhou University (January 2018–January 2024) was analyzed. Samples from 10 healthy individuals from the medical examination center served as controls. All materials were anonymized archival specimens, and the Ethics Review Committee granted exemption from informed consent (LDYYLL-2025-82).

Isolation of Peripheral Blood Mononuclear Cells (PBMCs)

Blood in EDTA tubes was centrifuged at 3000 rpm for 5 minutes at room temperature. Serum was removed, and PBMCs were isolated using Ficoll-Paque gradient centrifugation (Solarbio, P8610). Cells were stored at −80 °C until analysis.

Cell culture and treatment

Kasumi-1 (ATCC), HL60 (Wuhan Servicebio), and MOLM13 (provided by Dr. Shuling Zhang, First Affiliated Hospital of Lanzhou University) AML cell lines were maintained in RPMI 1640 supplemented with 10% fetal bovine serum and 1% penicillin-streptomycin at 37 °C and 5% CO_2. Mycoplasma testing (isothermal amplification, Servicebio) was negative for all lines.

HL60 cells received 3 μM or 6 μM decitabine (DAC) (TargetMol, Shanghai, China). MOLM13 cells were exposed to 5 μM SC79 and 10 μM BIP-V5 (TargetMol, Shanghai, China).

Lentiviral transfection

Kasumi-1, HL60, and MOLM13 cells were distributed into 24-well plates at 5×10^4 cells per well. Lentiviral vectors designed to enforce LINC01128 or TRIM58 expression, along with their respective shRNA constructs and matching negative controls (GeneChem, Shanghai, China), were introduced into each cell line. Prior pilot tests were carried out to determine the optimal multiplicity of infection, after which an MOI of 50 was selected as the standard condition. Following viral delivery, puromycin was applied for 72 hours and subsequently lowered to a maintenance dose to sustain stable polyclonal populations. Successful integration was confirmed using qPCR and Western blotting.

RNA isolation and quantification

Total RNA was harvested using the M5 Universal RNA Mini Kit (Mei5bio, Beijing, China). Concentration and purity assessments were made on a NanoDrop One spectrophotometer (Thermo Fisher Scientific, Waltham, MA, USA). cDNA synthesis employed the Hifair® III First Strand cDNA Synthesis SuperMix for qPCR (Yeasen, Shanghai, China). Amplification reactions were run on the QuantStudio 3 system using Hieff® qPCR SYBR Green Master Mix (Yeasen). Primer sets, purchased from Servicebio Biotechnology (Wuhan, China), were used for quantification. Expression levels were computed via the $2^{-}\Delta\Delta Cq$ procedure, normalizing first to GAPDH and then to the control group. Each sample included three technical replicates.

RNA sequencing (RNA-Seq)

Sequencing libraries were processed on the Illumina NovaSeq 6000. Read trimming was performed with Trimmomatic, and Fastp was used for additional filtering to retain clean reads. Differential expression analysis was executed using DESeq2, with transcripts meeting $p < 0.05$ and $|\log_2(\text{fold change})| > 0.58$ considered significant.

Methylation-specific PCR (MSP)

Genomic DNA was isolated with the M5 HiPer Universal DNA Mini Kit and treated using the EpiJET Bisulfite Conversion Kit. MSP reactions (MSP Kit) were run and examined on agarose gels.

Western blot analysis

Total protein from cultured cells or tissues was extracted using RIPA buffer. Samples were resolved via SDS-PAGE (1 hour) and transferred to PVDF membranes. Overnight incubation with primary antibodies at 4 °C was followed by HRP-linked secondary antibodies. Blots were visualized using a VILBER chemiluminescent imaging system (France). Antibodies were: anti-TRIM58 (1:1000, YT6944, Immunoway, USA), anti-GAPDH (1:8000, 60004-1-Ig, Proteintech, USA), anti-AKT (1:1000, 4691, CST, USA), anti-p-AKT (Ser473) (1:2000, 4060, CST, USA), anti-BAX (1:1000, 2772, CST, USA), and anti-BCL-2 (1:1000, 3498, CST, USA). Relative signal intensities were quantified using ImageJ 1.54f.

Subcellular fractionation

Isolation of cytoplasmic and nuclear RNA fractions was carried out with a nucleoplasmic separation kit from Beibei Biotechnology (Zhengzhou, China) according to the provided protocol.

Methylation-Sensitive Restriction Enzyme–qPCR (MSRE-qPCR)

MSRE-qPCR assays were conducted with the EpiJET DNA Methylation Analysis Kit (Thermo Fisher Scientific, Waltham, MA, USA). Genomic DNA was purified using the M5 HiPer Universal DNA Mini Kit (Mei5bio, Beijing, China). For each condition, 1 μg DNA was subjected to enzyme digestion, incubated at 37 °C for 1 hour, and heat-inactivated at 90 °C for 10 minutes. The proportion of 5-methylcytosine (5-mC) was calculated using the manufacturer's formula.

$$5-\mathrm{mC\ content}(\%) = \frac{100}{2^{\ C_{\mathrm{qHpaH-}} - C_{\mathrm{q\ undigested}}}} \quad (1)$$

Dual luciferase reporter assay

Reporter constructs were generated by inserting either the unaltered or mutated TRIM58 promoter fragments into the pGL3-basic backbone, together with the pcDNA3.1 plasmid carrying LINC01128. Genecreate Biological Engineering Co. (Wuhan, China) assembled these vectors. 293T cultures were co-transfected with the indicated plasmids using Lipofectamine 3000. After a 48-h incubation, luminescence was quantified using the Dual-Luciferase Reporter Assay System from Biosino Biotechnology and Science Inc (China), and Renilla activity served as the internal calibrator.

Chromatin immunoprecipitation (ChIP)

A ChIP kit (Beyotime, China) was used to evaluate DNMT1 occupancy on the TRIM58 promoter. Kasumi-1/MOLM13 cells were cross-linked with 37% formaldehyde for 10 min and quenched with glycine. Following cell disruption, chromatin was fragmented (40 W, 30 cycles, 10 s pulse/20 s pause) using a Scientz-IID sonicator (Ningbo, China) to yield 200–1000 bp products. Protein A+G agarose combined with salmon sperm DNA was pre-incubated to limit nonspecific interactions. Samples were then rotated at 4 °C overnight with anti-DNMT1 antibody (ab188453, Abcam, USA); normal IgG (30000-0-AP, Proteintech, USA) was used as a control. Complexes were captured with Protein A+G agarose/salmon sperm DNA for 60 min at 4 °C, followed by serial washes in low-salt, high-salt, LiCl, and TE buffers. Bound material was eluted (1% SDS, 0.1 M $NaHCO_3$), decross-linked in 5 M NaCl for 4 h at 65 °C, purified, and quantified by qPCR. Results are reported as enrichment relative to IgG.

RNA immunoprecipitation (RIP)

To determine DNMT1–LINC01128 RNA interactions, RIP was performed using the Geneseed kit (P0101, China). Magnetic beads were prepared and coupled to either anti-DNMT1 (ab188453, Abcam, USA) or IgG (30000-0-AP, Proteintech, USA). Cell lysates were incubated with the antibody-bound beads at 4 °C overnight. After the wash steps, RNA recovery was performed using spin column extraction and assessed by qPCR.

Cell counting kit-8 (CCK-8)

Cells at ~80% confluence in exponential growth were enumerated and plated at 2×10^4 cells per well in 96-well plates (100 μL medium each). After a 24-h culture period, 10 μL of CCK-8 reagent was added and incubated for 2 h at 37 °C in the dark. Absorbance at 450 nm was recorded using a BioTek Synergy Neo2 microplate reader (USA).

Apoptosis and cell cycle analysis

Apoptotic fractions were determined with the Annexin V-APC/7-AAD kit (Elabscience Biotechnology, Wuhan, China). Cells were stained for 15 min with Annexin V-APC and 7-AAD and examined by flow cytometry with the appropriate excitation/emission settings. For cell cycle profiling, the MultiSciences Biotech (Hangzhou, China) Cell Cycle Staining Kit was used. Cells were fixed, treated with propidium iodide in permeabilization buffer, and analyzed at low flow rates.

Xenograft tumor models

A total of twenty female NOD/SCID mice (5 weeks old, 18–22 g) were obtained from Changzhou Cavens Laboratory Animal Co. Each experimental group contained three or four animals. To induce tumors in the TRIM58-overexpression cohort, 4×10^6 MOLM13 cells suspended in 100 μL PBS were implanted subcutaneously in the right flank. For HL60 models, 5×10^6 cells were injected into the right inguinal site. Beginning on day 7 after implantation, the HL60 group received MLN4924 at 60 mg/kg via daily intraperitoneal administration for 14 days. Tumors were monitored every three days with calipers, and volumes were calculated using the standard formula:

$$v = 1/2 \times \text{Length} \times \text{width}^2 \quad (2)$$

The Ethics Committee limited allowable tumor size to 1500 mm^3, and throughout the experiment, no animal reached this volume. All mice were humanely sacrificed by CO_2 exposure exactly 3 weeks after tumor implantation. The resulting xenografts were removed and weighed for downstream evaluations.

Immunohistochemistry

Tumor samples were first held at 60 °C for 2 h, then subjected to deparaffinization and rehydration steps. Antigen retrieval was performed using a citrate-based solution. Endogenous peroxidase activity was blocked by treating the sections with 3% hydrogen peroxide for 10 min at room temperature. To reduce nonspecific binding, slides were incubated with 5% normal goat serum for 30 min before the addition of primary antibodies, which were applied overnight at 4 °C. After washing, HRP-linked secondary antibodies were introduced, followed by color formation with DAB and counterstaining with hematoxylin. Antibodies were used at the following dilutions: anti-PCNA (1:1000, Servicebio), anti-BCL-2 (1:500, Servicebio), anti-BAX (1:500, Servicebio), anti-AKT (1:200, CST), and anti-pAKT (1:300, CST).

Statistical analysis

Quantitative data were processed using GraphPad Prism 10.2 and R 4.0.3. Two-group comparisons relied on an unpaired Student's t-test. When more than two groups were analyzed, one-way ANOVA followed by Dunnett's post-test was used. All measurements are presented as mean ± SD. Statistical thresholds were defined as: $p < 0.05$, $p < 0.01$, $p < 0.001$, $p < 0.0001$.

Results and Discussion

MLN4924 and DAC remove methylation at the TRIM58 proximal promoter and elevate its expression

Earlier work with 850K methylation arrays showed that MLN4924 produced broad methylation shifts in AML cells and specifically reduced methylation at the cg26052730 locus within the TRIM58 promoter. Transcriptome sequencing simultaneously indicated that TRIM58 transcription increased following MLN4924 treatment. In the present experiments, Western blotting confirmed MLN4924-induced enhancement of TRIM58 protein in AML lines **(Figure 1a)**. These observations suggest that lowering methylation at this promoter region relieves transcriptional suppression and promotes TRIM58 protein synthesis.

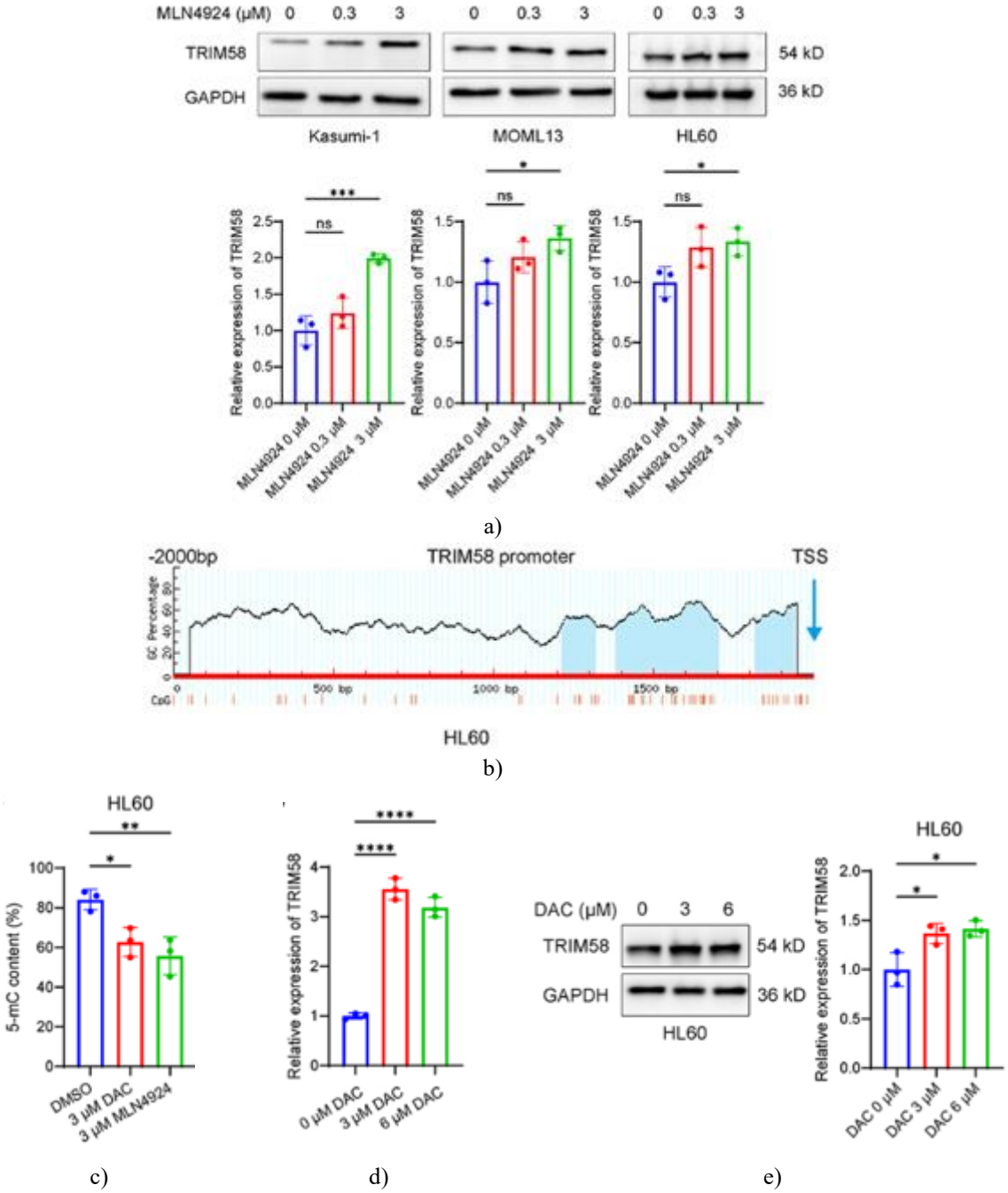

Figure 1. MLN4924 and DAC decrease methylation in the TRIM58 promoter and augment expression.
(a) Western blot showing TRIM58 protein in Kasumi-1, MOLM13, and HL60 cells exposed to 0, 0.3, or 3 μM MLN4924.
(b) Identification of CpG islands via MethPrimer.
(c) MSRE-qPCR assessment of 5-mC in the −182 to −58 CpG island of HL60 cells treated with 3 μM MLN4924 or 3 μM DAC for 24 h.
(d) RT-qPCR of TRIM58 after DAC exposure at multiple doses.
(e) Western blot verifying TRIM58 levels in HL60 cells treated with 0, 3, or 6 μM DAC. Data = mean ± SD; significance as stated (*p < 0.05; **p < 0.01; ***p < 0.0001).

MethPrimer [25] predicted three CpG islands in the TRIM58 promoter **(Figure 1b)**: spanning −785 to −683, −615 to −294, and −182 to −58 from the TSS. The methylation site cg26052730 (positions −156 to −155) lies within the closest island to the TSS. To assess how this region affects TRIM58 expression, primers were designed against this island and MSRE-qPCR was performed using HpaII (methylation-dependent) and MspI (methylation-independent). Significant loss of 5-mC was detected after MLN4924 or DAC treatment **(Figure 1c)**. DAC

additionally elevated TRIM58 transcripts and protein abundances in HL60 cells **(Figures 1d and 1e)**. Altogether, both drugs induce demethylation of this promoter island and increase TRIM58 expression.

TRIM58 restricts AML cell growth and facilitates apoptosis in vitro

Since TRIM58 has been implicated as a tumor-suppressive gene, its function in AML was examined. GEO dataset analysis showed markedly reduced expression in AML relative to healthy samples **(Figure 2a)**. Peripheral blood from 17 AML patients and 10 controls further verified this reduction **(Figure 2b)**.

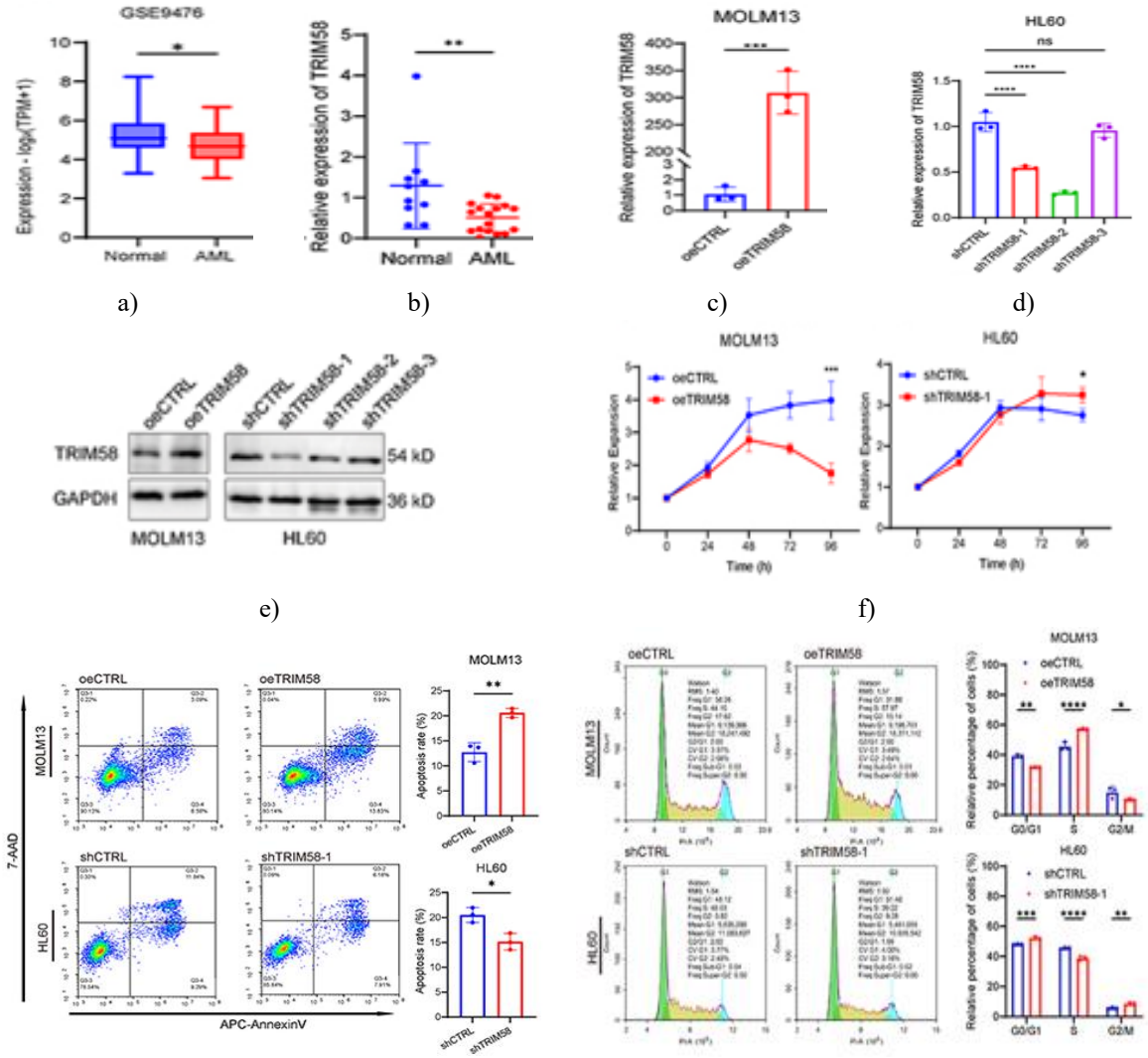

a) b) c) d) e) f) g) h)

Figure 2. TRIM58 suppresses proliferation and promotes apoptosis in AML cells.
(a) TRIM58 levels in AML (n = 26) vs. healthy controls (n = 38) using dataset GSE9476.
(b) RT-qPCR in controls (n = 10) vs. AML patients (n = 17).
(c–d) RT-qPCR confirming TRIM58 overexpression in MOLM13 and knockdown in HL60.
(e) Western blot validating altered TRIM58 expression in the same lines.
(f) CCK-8-based proliferation assays following TRIM58 upregulation or depletion.
(g–h) Flow-cytometric evaluation of apoptosis and cell-cycle profiles 7 days after transfection. Data = mean ± SD; significance as above.
Abbreviation: ns = not significant.

We established stable TRIM58-overexpressing MOLM13 cells and TRIM58-silenced HL60 cells using lentiviral transduction, and confirmed the efficiency of both manipulations **(Figures 2c–2e)**. CCK-8 analysis showed that elevating TRIM58 levels reduced cell growth, whereas TRIM58 depletion enhanced proliferative capacity **(Figure 2f)**. To further clarify how TRIM58 influences AML cell expansion, apoptosis, and cell-cycle status were

evaluated by flow cytometry. Overexpressing TRIM58 increased apoptotic rates, while its knockdown diminished apoptosis **(Figure 2g)**. In addition, TRIM58 overexpression led to a higher percentage of cells in S phase, whereas loss of TRIM58 resulted in a reduced S-phase population **(Figure 2h)**. The same series of assays performed in Kasumi-1 cells produced comparable results for proliferation and apoptosis, although TRIM58 modulation had no marked influence on cell-cycle distribution.

MLN4924 triggers apoptosis by acting through the TRIM58/AKT/BAX cascade

Given that heightened TRIM58 expression promotes apoptosis in AML cells, we next examined the relationship between TRIM58 and the apoptosis-associated proteins BCL-2 and BAX. TRIM58 overexpression elevated BAX protein levels without noticeably affecting BCL-2 **(Figure 3a)**. Because AKT is known to suppress BAX via the intrinsic mitochondrial pathway [26], we investigated whether TRIM58 alters AKT activity. The data indicated lower p-AKT levels in TRIM58-overexpressing cells, while total AKT remained unchanged **(Figure 3a)**. This suggests that TRIM58 reduces AKT signaling by limiting AKT phosphorylation, thereby enabling BAX upregulation.

Since MLN4924 is also capable of inhibiting AKT phosphorylation, we conducted a rescue experiment to determine whether TRIM58 is required for this effect. Compared with MLN4924 alone, silencing TRIM58 counteracted MLN4924-mediated suppression of AKT signaling and simultaneously enhanced cell growth while decreasing apoptosis **(Figures 3b–3f)**.

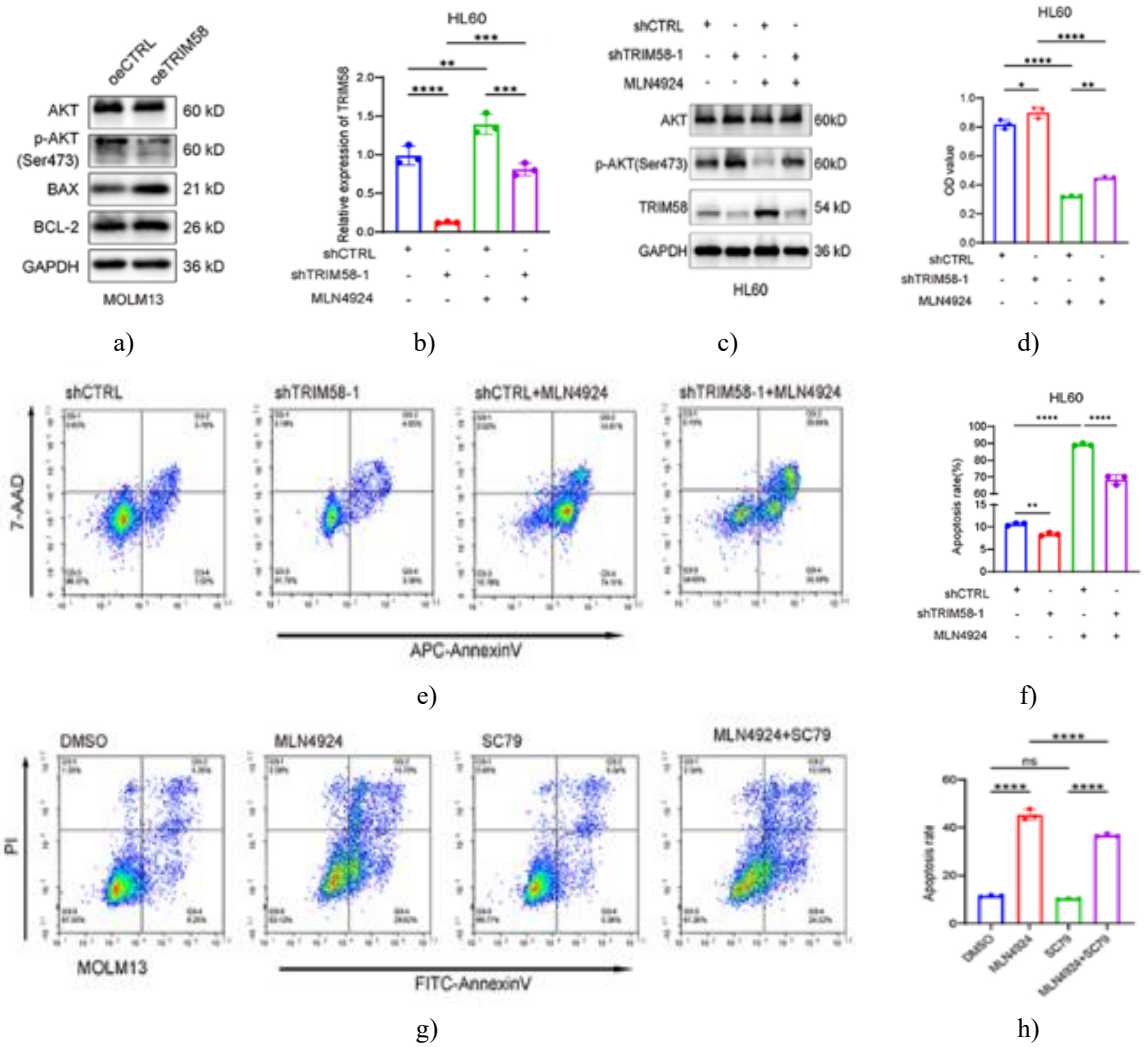

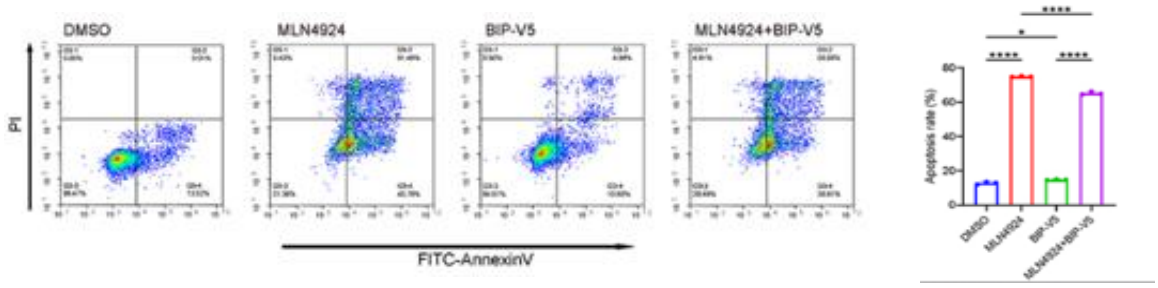

i) j)

Figure 3. MLN4924 promotes apoptosis via the TRIM58/AKT/BAX pathway.
(a) Western blot of AKT-related proteins, BCL-2, and BAX in TRIM58-overexpressing MOLM13 cells.
(b) RT-qPCR assessment of TRIM58 expression in each group.
(c) Western blot of AKT, p-AKT, and TRIM58.
(d) CCK-8–based viability at 450 nm.
(e–f) Flow-cytometric apoptosis analysis across groups.
(g–h) Apoptosis in MOLM13 cells exposed to DMSO, MLN4924 (0.3 μM), SC79 (5 μM), or MLN4924 + SC79.
(i–j) Apoptosis in MOLM13 cells treated with DMSO, MLN4924 (0.3 μM), BIP-V5 (10 μM), or MLN4924 + BIP-V5.
Data = mean ± SD. *p < 0.05; **p < 0.01; ***p < 0.001; ****p < 0.0001.

To further determine whether MLN4924-induced apoptosis depends on the TRIM58/AKT/BAX axis, we used the AKT activator SC79 and the BAX inhibitor BIP-V5. SC79 activation markedly weakened MLN4924-induced apoptosis **(Figures 3g and 3h)**, and BIP-V5 treatment similarly reduced the apoptotic response to MLN4924 **(Figures 3i and 3j)**. Together, these findings demonstrate that MLN4924 drives apoptosis partly by modulating the TRIM58/AKT/BAX signaling pathway.

MLN4924 Administration and TRIM58 Overexpression Suppress AML Progression in vivo by Inhibiting AKT

We next investigated the in vivo antitumor effects of MLN4924 and TRIM58 overexpression using a subcutaneous AML xenograft model. Tumor size and weight were markedly decreased in MLN4924-treated mice relative to controls **(Figures 4a–4c)**. Animals implanted with TRIM58-overexpressing MOLM13 cells also developed smaller tumors with lower final tumor weight **(Figures 4d–4f)**. MLN4924 elevated TRIM58 and BAX protein expression while reducing PCNA, BCL-2, and p-AKT levels **(Figures 4g and 4h)**. Consistently, TRIM58 overexpression increased BAX while lowering PCNA and p-AKT, though BCL-2 and total AKT were largely unaffected **(Figure 4i)**. These results indicate that both MLN4924 and TRIM58 impair AML tumor growth in vivo by downregulating AKT signaling.

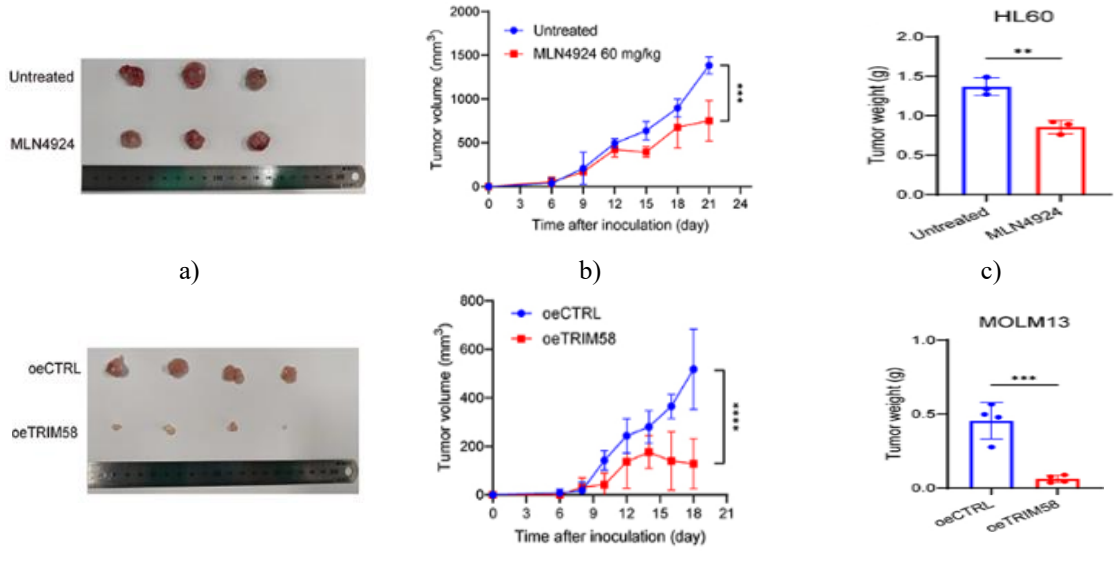

a) b) c)

d) e) f)

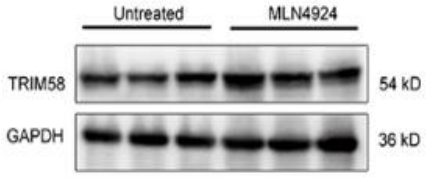

g)

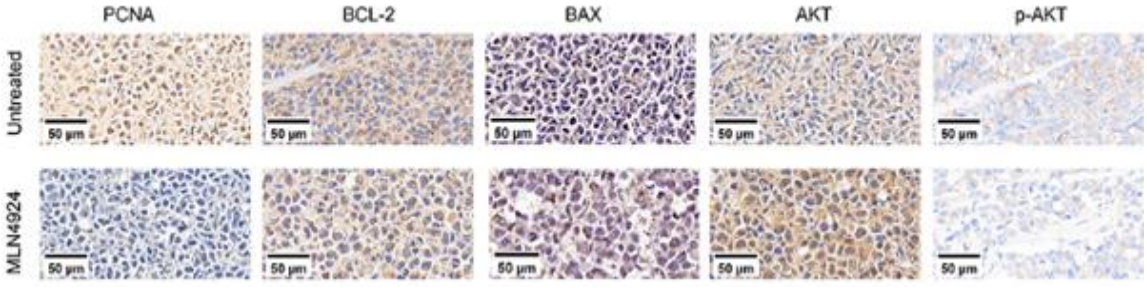

h)

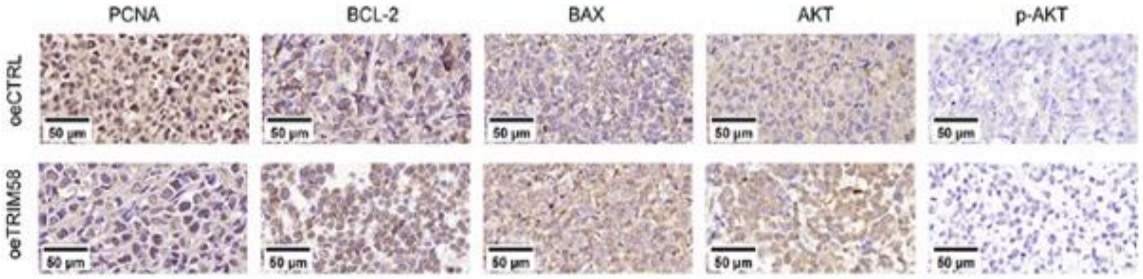

i)

Figure 4. MLN4924 suppresses AML cell proliferation through TRIM58 upregulation in vivo.
(a–c) Tumor volume and mass comparison between untreated and MLN4924-treated mice.
(d–f) Tumor volume and mass comparison between control and TRIM58-overexpressing groups.
(g) Western blot detection of TRIM58 in MLN4924-treated vs. control tumors.
(h–i) IHC staining of PCNA, BCL-2, BAX, AKT, and p-AKT in all four groups. Scale bar: 50 μm.
Data = mean ± SD. **p < 0.01; ***p < 0.001; ****p < 0.0001.

LINC01128 regulates MLN4924-induced TRIM58 upregulation in AML

Because lncRNAs are known to influence DNA methylation in various biological settings, we explored MLN4924-responsive lncRNAs that might regulate TRIM58. RNA-seq performed on Kasumi-1 cells treated with MLN4924 or DMSO for 24 h identified 2553 differentially expressed lncRNAs **(Figures 5a and 5b)**. Focusing on the top 500 lncRNAs ranked by |log2FC|, we queried the Multi-Experiment Matrix (MEM) database [27]. Among them, LINC01128 and CYTOR showed the strongest positive association with TRIM58 expression **(Figure 5c)**.

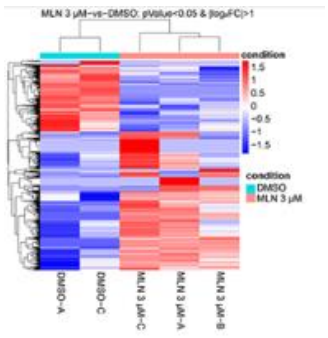

a)

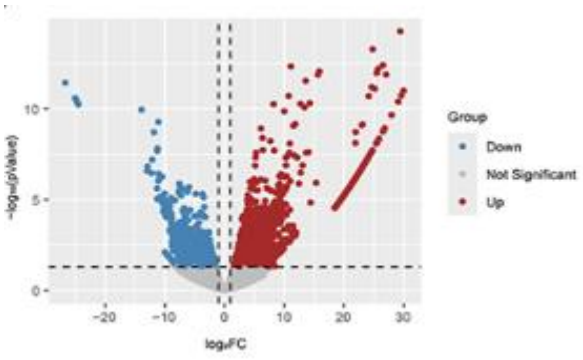

b)

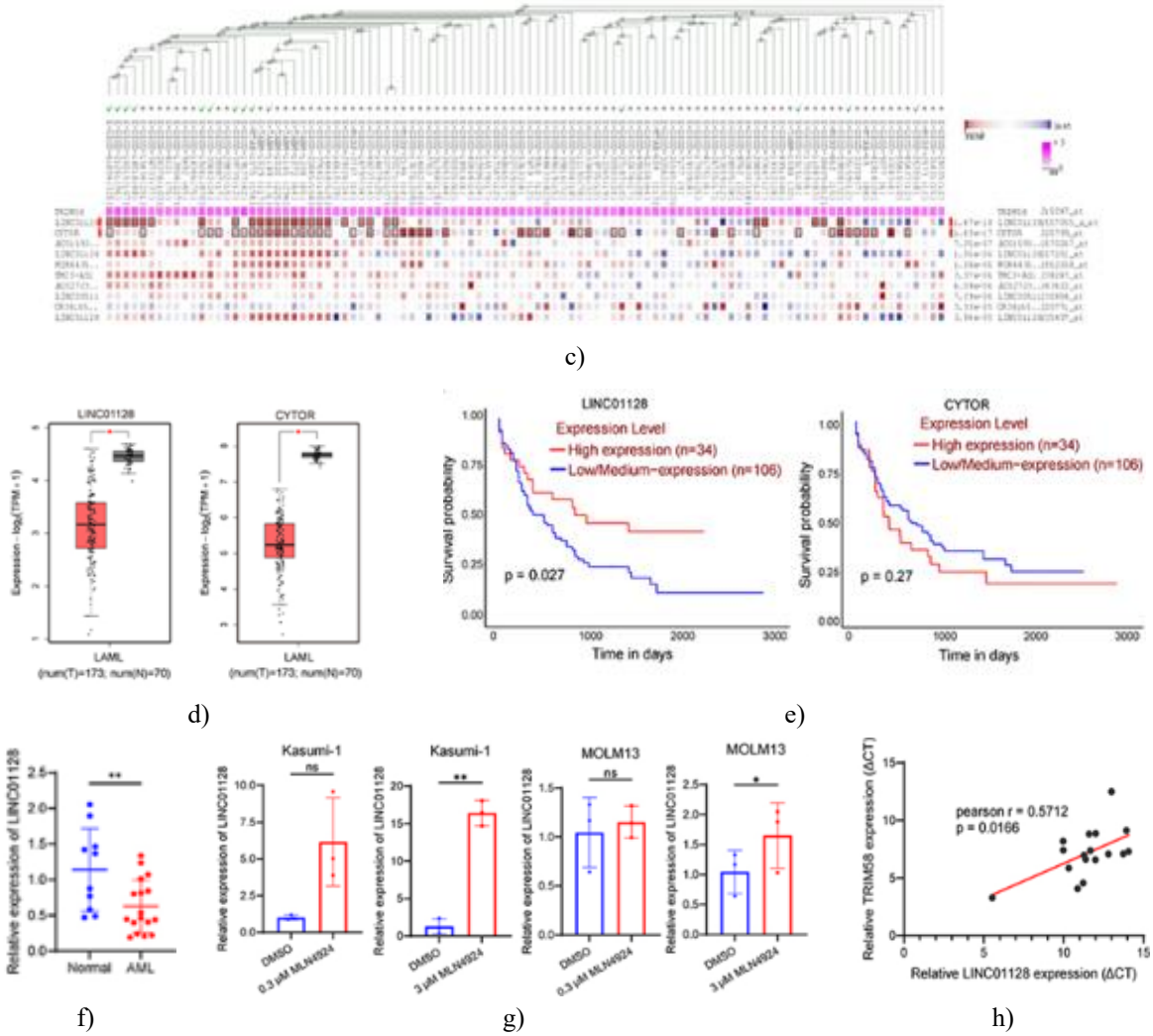

Figure 5. RNA-seq combined with co-expression resources highlights lncRNAs that participate in MLN4924-driven elevation of TRIM58.

(a) A heat map displays the lncRNA expression shifts between cells receiving 3 μM MLN4924 and those treated with 0.1% DMSO, where red marks higher and blue marks lower transcript abundance.

(b) A volcano representation summarizes lncRNA alterations under the same treatment conditions.

(c) MEM-based correlation mapping shows how these altered lncRNAs relate to TRIM58, with red indicating positive associations and blue indicating negative ones.

(d) GEPIA output illustrating LINC01128 and CYTOR expression patterns in AML compared with healthy samples.

(e) Kaplan–Meier survival charts stratifying AML patients by the median expression of LINC01128 or CYTOR.

(f) RT-qPCR evaluation of LINC01128 in healthy individuals (n = 10) versus AML cases (n = 17).

(g) RT-qPCR measurement of LINC01128 following MLN4924 exposure in Kasumi-1 and MOLM13.

(h) Spearman's association between LINC01128 and TRIM58 in AML (n = 17). Values shown as mean ± SD. *p < 0.05; *p < 0.01.

ns = not significant.

RNA-seq profiling revealed that LINC01128 and CYTOR rise following MLN4924 treatment. Their expression and outcome relevance were then queried using GEPIA and UALCAN, showing that both transcripts appear lower in AML relative to normal samples **(Figures 5c and 5d)**. Notably, diminished LINC01128 corresponded to reduced survival, whereas CYTOR lacked prognostic weight (log-rank p = 0.27, **(Figure 5e)**). RT-qPCR further demonstrated that LINC01128 is markedly reduced in AML **(Figure 5f)**, while MLN4924 exposure prominently

elevated its expression in AML cell lines **(Figure 5g)**. A significant positive link between LINC01128 and TRIM58 was also detected (Pearson r = 0.5712, p = 0.0166, **(Figure 5h)**).
Altogether, these observations imply that MLN4924 may enhance TRIM58 levels through the induction of LINC01128 within AML.

LINC01128 restrains AML progression through the AKT/BAX signaling axis
To determine how LINC01128 influences AML phenotypes, lentiviral systems enabling its overexpression or depletion were generated in MOLM13 and HL60, and modulation efficiency was validated **(Figure 6a)**. CCK-8 assays indicated no proliferative effect from overexpression, but silencing LINC01128 resulted in increased cell growth **(Figure 6b)**. Flow cytometry showed that elevated LINC01128 strengthens apoptosis, whereas its knockdown reduces apoptotic activity **(Figure 6c)**. Cell-cycle analysis revealed S-phase enrichment after overexpression and a notable S-phase reduction following knockdown **(Figure 6d)**. Comparable findings were recorded in Kasumi-1 cells, where overexpression also uniquely slowed proliferation.

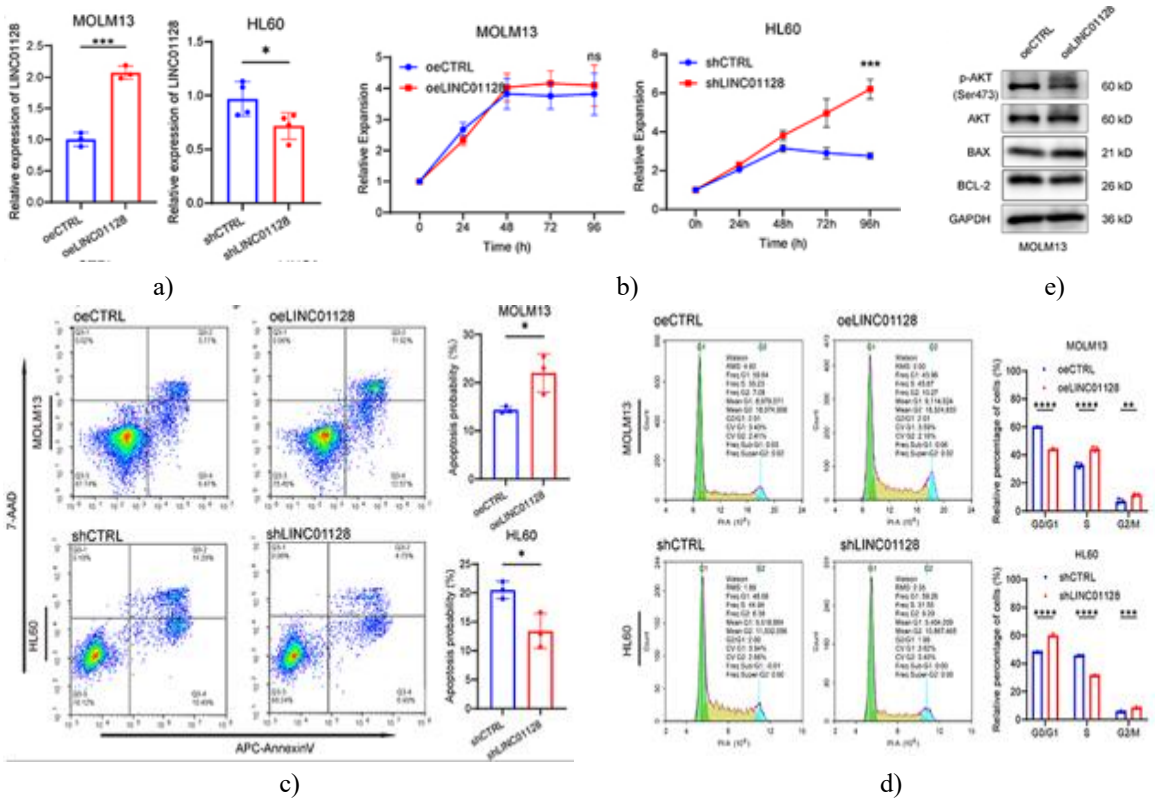

Figure 6. LINC01128 enhancement promotes apoptosis in AML cells, while its depletion produces the reverse outcome.
(a) RT-qPCR confirmation of LINC01128 overexpression in MOLM13 and knockdown in HL60.
(b) CCK-8 proliferation measurements under both conditions.
(c–d) Flow cytometric quantification of apoptosis and cell-cycle profiles.
(e) Western blot detection of AKT-related components, BCL-2, and BAX in MOLM13 overexpressing LINC01128. Data are mean ± SD. *p < 0.05; **p < 0.01; ***p < 0.001; ***p < 0.0001.
ns = not significant.

Analysis of downstream pathways showed that enforcing LINC01128 expression diminished p-AKT and BCL-2, increased BAX, and produced minimal variation in total AKT **(Figure 6e)**. These molecular changes indicate inhibition of AKT signaling and reinforcement of pro-apoptotic activity.
Thus, LINC01128 limits AML cell expansion and enhances apoptosis in a manner analogous to TRIM58.

DNMT1 Retention by LINC01128 Promotes TRIM58 Demethylation and Transcriptional Reactivation
Because lncRNAs often influence tumor biology by directing DNA-methylation dynamics, we next examined the functional attributes of LINC01128 in AML. Computational localization using lncATLAS suggested that

LINC01128 predominantly resides in the nucleus across most examined cell lines, with mixed nuclear–cytoplasmic presence in K562 **(Figure 7a)**. Additional support from RNALOCATE confirmed its largely nuclear enrichment in THP-1 and K562. Nucleus–cytoplasm fractionation followed by RT-qPCR further validated this distribution pattern **(Figure 7b)**.

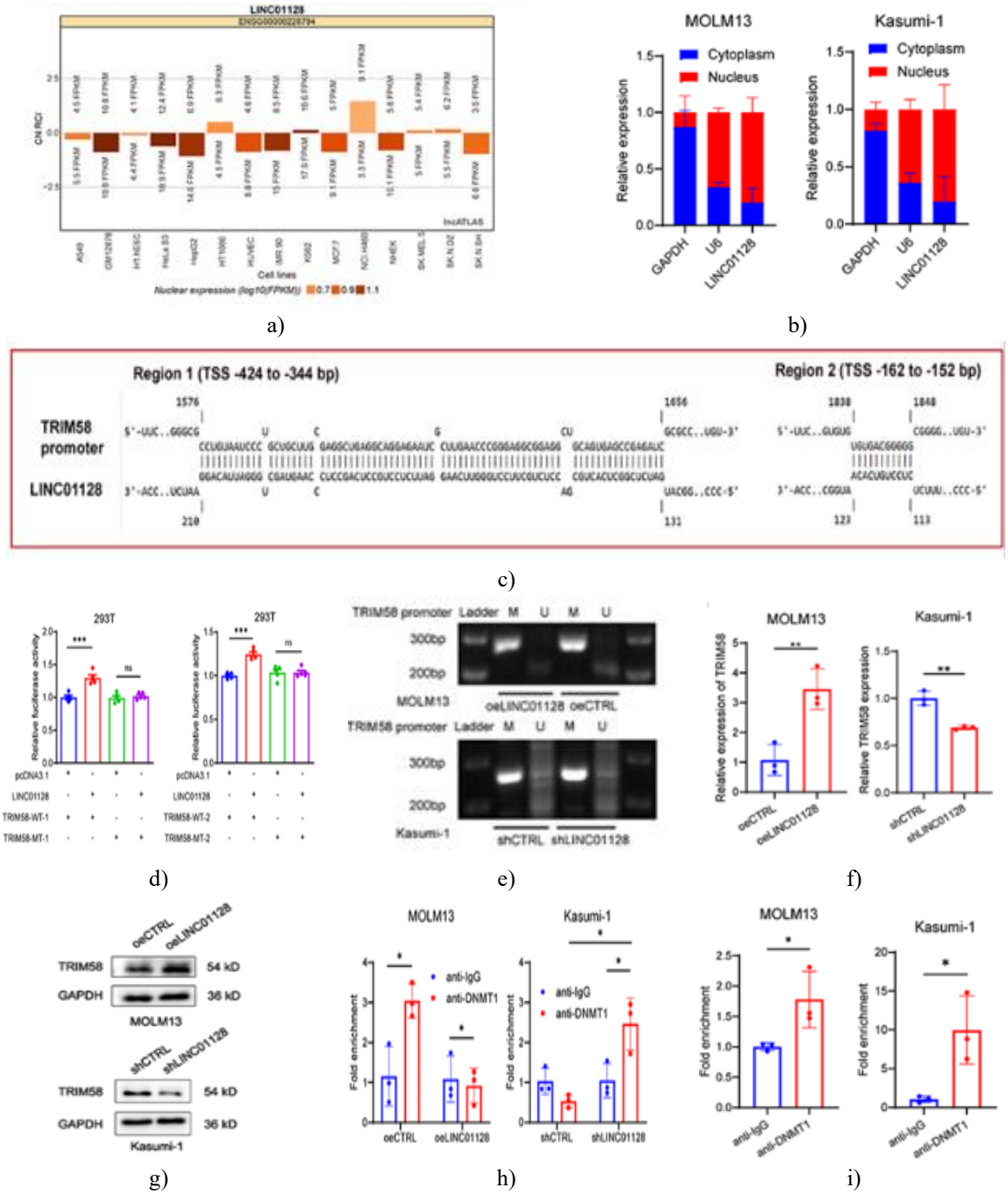

Figure 7. LINC01128 interacts with DNMT1 and restricts its access to the TRIM58 promoter, limiting DNMT1-dependent methylation.

(a) Subcellular positioning of LINC01128 predicted via lncATLAS.

(b) RT-qPCR performed on separated nuclear and cytoplasmic fractions showed that LINC01128 RNA is mainly nuclear in Kasumi-1 and MOLM-13 cells.

(c) IntaRNA analysis identified putative contact regions between LINC01128 and the TRIM58 promoter.

(d) Dual-luciferase assays confirmed that LINC01128 associates with the TRIM58 promoter.

(e) MSP profiling demonstrated shifts in TRIM58 promoter methylation following altered LINC01128 expression. M: methylated; U: unmethylated.

(f) RT-qPCR quantification of TRIM58 transcripts after LINC01128 upregulation in MOLM13 or knockdown in HL60.
(g) Western blot evaluation of TRIM58 protein under the same conditions.
(h) ChIP analysis examined how LINC01128 overexpression or silencing affects DNMT1 occupancy at the TRIM58 promoter.
(i) RIP assays verified direct binding between DNMT1 and LINC01128. Values are presented as mean ± SD. *p < 0.05; **p < 0.01; ***p < 0.001.
Abbreviation: ns, not significant.

IntaRNA predicted two interaction sites between LINC01128 and the proximal TRIM58 promoter **(Figure 7c)**, and reporter assays validated this prediction **(Figure 7d)**. Elevating LINC01128 induced hypomethylation within the proximal TRIM58 promoter **(Figure 7e)**, accompanied by increased transcript and protein levels **(Figures 7f and 7g)**. Conversely, suppressing LINC01128 produced promoter hypermethylation **(Figure 7e)** and lowered TRIM58 expression **(Figures 7f and 7g)**.
Since DNMT1 is the principal methyltransferase responsible for silencing tumor suppressor loci during DNA replication [28], we considered its potential role in TRIM58 regulation. ChIP experiments revealed that DNMT1 occupancy at TRIM58 diminished when LINC01128 was overexpressed, but increased when LINC01128 was depleted **(Figure 7h)**. RIP assays in MOLM13 and Kasumi-1 confirmed a physical association between DNMT1 and LINC01128 **(Figure 7i)**.
Overall, these observations indicate that LINC01128 restricts DNMT1 from engaging the TRIM58 promoter, likely through sequestration or competitive interaction.

TRIM58 knockdown counteracts LINC01128-driven growth suppression and apoptosis in AML
To evaluate whether TRIM58 is required for LINC01128-mediated regulation of AML proliferation and apoptosis, we performed rescue assays in HL60 cells. The CCK-8 assay showed that LINC01128 overexpression markedly reduced cell growth relative to the control, whereas simultaneous TRIM58 knockdown restored proliferation **(Figures 8a and 8b)**.

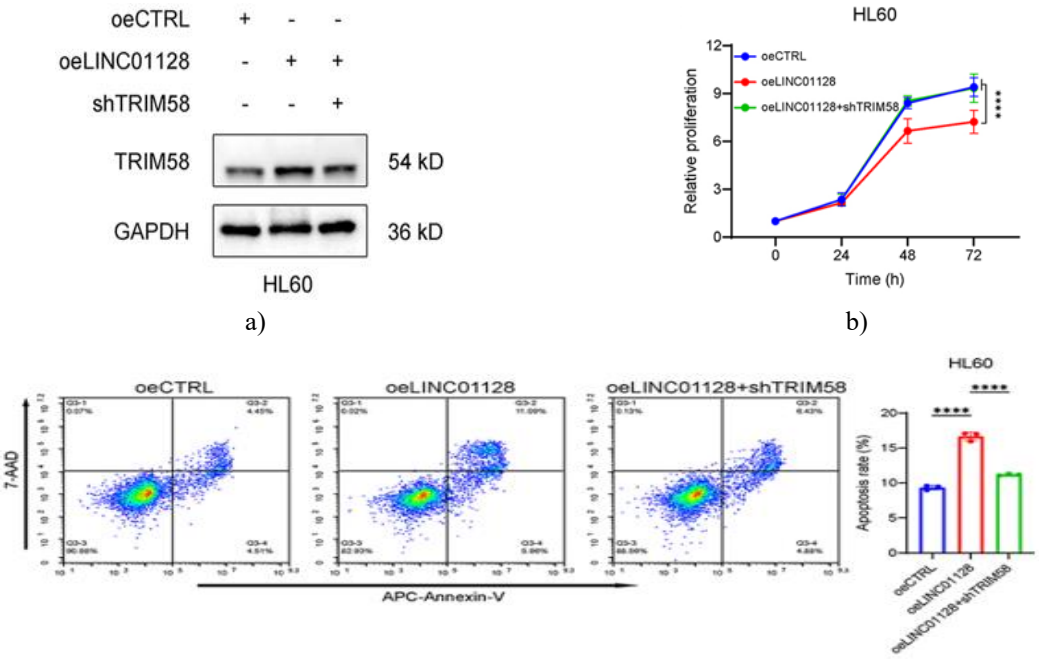

Figure 8. TRIM58 silencing negates the tumor-inhibitory effects of LINC01128 in AML cells.
(a) TRIM58 protein abundance in oeCTRL, oeLINC01128, and oeLINC01128 + shTRIM58 groups.
(b) Cell viability (450 nm) assessed by CCK-8 across groups.
(c) Flow cytometric quantification of apoptosis. Data represented as mean ± SD. ****p < 0.0001.

Apoptosis analysis showed that LINC01128 overexpression substantially increased programmed cell death compared with controls, whereas co-silencing of TRIM58 weakened this pro-apoptotic response **(Figure 8c)**. These data indicate that TRIM58 is a crucial downstream effector of LINC01128.

Although therapeutic strategies for AML have progressed, overall outcomes remain unsatisfactory. Aberrant promoter hypermethylation of tumor suppressor genes remains a major contributor to AML development, prompting efforts to identify effective demethylating approaches. In earlier work, we observed that the ubiquitin-like pathway blocker MLN4924 altered the epigenetic landscape of AML cells, notably inducing substantial demethylation of the TRIM58 promoter, and that excessive promoter methylation correlated with unfavorable clinical outcomes. In this study, we further explored TRIM58's role in AML and clarified how MLN4924 influences its methylation status. Our findings indicate that MLN4924 elevates LINC01128, which in turn prevents DNMT1 engagement, thereby restoring TRIM58 expression and triggering reduced cell proliferation accompanied by increased apoptosis. This mechanism represents an additional layer of MLN4924's antileukemic activity.

Prior evidence indicates that TRIM58 functions as a tumor-inhibitory factor across multiple malignancies. In colorectal cancer, TRIM58 limits tumor growth and induces apoptosis by promoting RECQL4 ubiquitination and suppressing the AKT cascade [29]; in lung cancer, TRIM58 drives ZEB1 degradation through the ubiquitin–proteasome system, reducing tumor motility and survival [30]. Importantly, in hepatocellular carcinoma [22], lung adenocarcinoma [23], and renal cell carcinoma [24], TRIM58 expression is frequently diminished due to promoter hypermethylation, implying that epigenetic repression of TRIM58 may be widespread across cancers. Consistent with these reports, we identified markedly reduced TRIM58 expression in AML patients relative to healthy controls, accompanied by hypermethylation of its proximal promoter. Our results, therefore, position TRIM58 as a previously unrecognized tumor suppressor gene in AML. Mechanistically, TRIM58 overexpression hindered AML cell proliferation, triggered apoptosis, and altered BAX and p-AKT levels. Rescue analyses showed that reducing TRIM58 expression counteracted MLN4924-induced suppression of AKT signaling, supporting TRIM58's role as a downstream mediator of MLN4924.

Many published studies report that lncRNAs typically enhance promoter methylation by directing DNMTs to specific genomic loci. For instance, lncRNA-ZFAS1 binds the Notch1 promoter and recruits DNMT3b, increasing Notch1 methylation and aggravating myocardial ischemia/reperfusion injury [31]; similarly, lncRNA SNHG1 engages DNMT1 and DNMT3B at the ZCCHC10 promoter, inducing hypermethylation that promotes AML progression and venetoclax resistance [32], as well as vinblastine resistance. Unlike these mechanisms, we discovered an entirely different regulatory model: LINC01128 binds to and retains DNMT1, thereby preventing DNMT1-driven methylation of the TRIM58 promoter and allowing TRIM58 expression to recover. Functionally, LINC01128 acts as a tumor-suppressive lncRNA; its overexpression reduces AML cell proliferation and triggers apoptosis, associated with diminished p-AKT and BCL-2 and increased BAX. This pro-apoptotic capacity is consistent with previous work showing that nuclear LINC01128 induces cell death in THP-1 cells through NLRP3 engagement [33].

Interestingly, forced expression of either TRIM58 or LINC01128 interfered with cell-cycle progression, increasing the proportion of S-phase cells. Such S-phase accumulation is likely to initiate caspase-dependent cell death, suggesting that perturbations in DNA-replication checkpoints may contribute to their apoptotic effects. The precise cell-cycle regulators involved remain unidentified and warrant further investigation.

Although neddylation is widely recognized for modulating CRLs, recent studies have shown that several non-cullin E3 ligases—including VHL [34], Parkin [35], and MDM2—are also subject to this modification. Whether TRIM58, itself a non-cullin E3 ligase, undergoes similar neddylation-based control and whether such regulation contributes to its tumor-inhibitory properties remain open questions.

Conclusion

Overall, our work demonstrates that MLN4924 suppresses AML progression by restoring TRIM58 activity through LINC01128-mediated DNMT1 sequestration. This regulatory pathway provides new insights into the epigenetic actions of MLN4924 and highlights TRIM58 as a promising therapeutic target in AML.

Acknowledgments: None

Conflict of Interest: None

Financial Support: None

Ethics Statement: None

References

1. Forsberg M, Konopleva M. AML treatment: conventional chemotherapy and emerging novel agents. Trends Pharmacol Sci. 2024;45(5):430–48. doi:10.1016/j.tips.2024.03.005
2. Godfrey LC, Rodriguez-Meira A. Viewing AML through a new lens: technological advances in the study of epigenetic regulation. Cancers. 2022;14(23):5989. doi:10.3390/cancers14235989
3. Fu DJ, Wang T. Targeting NEDD8-activating enzyme for cancer therapy: developments, clinical trials, challenges and future research directions. J Hematol Oncol. 2023;16(1):87. doi:10.1186/s13045-023-01485-7
4. Zheng B, Qian F, Wang X, Wang Y, Zhou B, Fang L. Neddylation activated TRIM25 desensitizes triple-negative breast cancer to paclitaxel via TFEB-mediated autophagy. J Exp Clin Cancer Res. 2024;43(1):177. doi:10.1186/s13046-024-03085-w
5. Zhang Y, Du L, Wang C, Jiang Z, Duan Q, Li Y, et al. Neddylation is a novel therapeutic target for lupus by regulating double negative T cell homeostasis. Signal Transduct Target Ther. 2024;9(1):18. doi:10.1038/s41392-023-01709-9
6. Murthy GS, Saliba AN, Szabo A, Harrington A, Abedin S, Carlson K, et al. A Phase I study of pevonedistat, azacitidine, and venetoclax in patients with relapsed/refractory acute myeloid leukemia. Haematologica. 2024;109(9):2864–72. doi:10.3324/haematol.2024.285014
7. Short NJ, Muftuoglu M, Ong F, Nasr L, Macaron W, Montalban-Bravo G, et al. A Phase 1/2 study of azacitidine, venetoclax and pevonedistat in newly diagnosed secondary AML and in MDS or CMML after failure of hypomethylating agents. J Hematol Oncol. 2023;16(1):73. doi:10.1186/s13045-023-01476-8
8. Adès L, Girshova L, Doronin VA, Díez-Campelo M, Valcárcel D, Kambhampati S, et al. Pevonedistat plus azacitidine vs azacitidine alone in higher-risk MDS/chronic myelomonocytic leukemia or low-blast-percentage AML. Blood Adv. 2022;6(17):5132–45. doi:10.1182/bloodadvances.2022007334
9. Saliba AN, Kaufmann SH, Stein EM, Patel PA, Baer MR, Stock W, et al. Pevonedistat with azacitidine in older patients with TP53-mutated AML: a Phase 2 study with laboratory correlates. Blood Adv. 2023;7(11):2360–3. doi:10.1182/bloodadvances.2022008625
10. Fathi AT. Pevonedistat, a new partner for 5-azacitidine. Blood. 2018;131(13):1391–2. doi:10.1182/blood-2018-02-829051
11. Visconte V, Nawrocki ST, Espitia CM, Kelly KR, Possemato A, Beausoleil SA, et al. Comprehensive quantitative proteomic profiling of the pharmacodynamic changes induced by MLN4924 in acute myeloid leukemia cells establishes rationale for its combination with azacitidine. Leukemia. 2016;30(5):1190–4. doi:10.1038/leu.2015.250
12. Handa H, Cheong JW, Onishi Y, Iida H, Kobayashi Y, Kim HJ, et al. Pevonedistat in East Asian patients with acute myeloid leukemia or myelodysplastic syndromes: a phase 1/1b study to evaluate safety, pharmacokinetics and activity as a single agent and in combination with azacitidine. J Hematol Oncol. 2022;15(1):56. doi:10.1186/s13045-022-01264-w
13. Schoofs T, Müller-Tidow C. DNA methylation as a pathogenic event and as a therapeutic target in AML. Cancer Treat Rev. 2011;37:S13–8. doi:10.1016/j.ctrv.2011.04.013
14. Zhang X, Zhang K, Zhang J, Chang W, Zhao Y, Suo X. DNMTs-mediated SOCS3 methylation promotes the occurrence and development of AML. Eur J Haematol. 2024;112(3):439–49. doi:10.1111/ejh.14134
15. Li T, Gao R, Xu K, Pan P, Chen C, Wang D, et al. BCL7A inhibits the progression and drug-resistance in acute myeloid leukemia. Drug Resist Updat. 2024;76:101120. doi:10.1016/j.drup.2024.101120
16. Patiño-Mercau JR, Baliñas-Gavira C, Andrades A, Benitez-Cantos MS, Rot AE, Rodriguez MI, et al. BCL7A is silenced by hypermethylation to promote acute myeloid leukemia. Biomark Res. 2023;11(1):32. doi:10.1186/s40364-023-00472-x

17. Patiño-Mercau JR, Baliñas-Gavira C, Andrades A, Benitez-Cantos MS, Rot AE, Rodriguez MI, et al. Decreased SCIN expression, associated with promoter methylation, is a valuable predictor for prognosis in acute myeloid leukemia. Mol Carcinog. 2018;57(6):735–44. doi:10.1002/mc.22794
18. Huang W, Li H, Yu Q, Xiao W, Wang DO. LncRNA-mediated DNA methylation: an emerging mechanism in cancer and beyond. J Exp Clin Cancer Res. 2022;41(1):100. doi:10.1186/s13046-022-02319-z
19. Hu X, Wu J, Feng Y, Ma H, Zhang E, Zhang C, et al. METTL3-stabilized super enhancers-lncRNA SUCLG2-AS1 mediates the formation of a long-range chromatin loop between enhancers and promoters of SOX2 in metastasis and radiosensitivity of nasopharyngeal carcinoma. Clin Transl Med. 2023;13(9):e1361. doi:10.1002/ctm2.1361
20. Qiannan D, Qianqian J, Jiahui S, Haowei F, Qian X. LncRNA PVT1 mediates the progression of liver necroptosis via ZBP1 promoter methylation under nonylphenol exposure. Sci Total Environ. 2022;844:157185. doi:10.1016/j.scitotenv.2022.157185
21. Guo Y, Jian J, Tang X, Zhao L, Liu B. Comprehensive analysis of DNA methylation and gene expression to identify tumor suppressor genes reactivated by MLN4924 in acute myeloid leukemia. Anticancer Drugs. 2025;36(3):199–207. doi:10.1097/cad.0000000000001688
22. Qiu X, Huang Y, Zhou Y, Zheng F. Aberrant methylation of TRIM58 in hepatocellular carcinoma and its potential clinical implication. Oncol Rep. 2016;36(2):811–8. doi:10.3892/or.2016.4871
23. Kajiura K, Masuda K, Naruto T, Kohmoto T, Watabnabe M, Tsuboi M, et al. Frequent silencing of the candidate tumor suppressor TRIM58 by promoter methylation in early-stage lung adenocarcinoma. Oncotarget. 2017;8(2):2890–905. doi:10.18632/oncotarget.13761
24. Gan Y, Cao C, Li A, Song H, Kuang G, Ma B, et al. Silencing of the TRIM58 gene by aberrant promoter methylation is associated with a poor patient outcome and promotes cell proliferation and migration in clear cell renal cell carcinoma. Front Mol Biosci. 2021;8:655126. doi:10.3389/fmolb.2021.655126
25. Li LC, Dahiya R. MethPrimer: designing primers for methylation PCRs. Bioinformatics. 2002;18(11):1427–31. doi:10.1093/bioinformatics/18.11.1427
26. Simonyan L, Renault TT, da Costa Novais MJ, Sousa MJ, Côrte-Real M, Camougrand N, et al. Regulation of Bax/mitochondria interaction by AKT. FEBS Lett. 2016;590(1):13–21. doi:10.1002/1873-3468.12030
27. Adler P, Kolde R, Kull M, Tkachenko A, Peterson H, Reimand J, et al. Mining for coexpression across hundreds of datasets using novel rank aggregation and visualization methods. Genome Biol. 2009;10(12):R139. doi:10.1186/gb-2009-10-12-r139
28. Wong KK, Lawrie CH, Green TM. Oncogenic roles and inhibitors of DNMT1, DNMT3A, and DNMT3B in acute myeloid leukaemia. Biomark Insights. 2019;14:1177271919846454. doi:10.1177/1177271919846454
29. Sun N, Shen J, Shi Y, Liu B, Gao S, Chen Y, et al. TRIM58 functions as a tumor suppressor in colorectal cancer by promoting RECQL4 ubiquitination to inhibit the AKT signaling pathway. World J Surg Oncol. 2023;21(1):231. doi:10.1186/s12957-023-03124-4
30. Shang R, Chen J, Gao Y, Chen J, Han G. TRIM58 interacts with ZEB1 to suppress NSCLC tumor malignancy by promoting ZEB1 protein degradation via UPP. Dis Markers. 2023;2023(1):5899662. doi:10.1155/2023/5899662
31. Li M, Jiao L, Shao Y, Li H, Sun L, Yu Q, et al. LncRNA-ZFAS1 promotes myocardial ischemia-reperfusion injury through DNA methylation-mediated Notch1 down-regulation in mice. JACC Basic Transl Sci. 2022;7(9):880–95. doi:10.1016/j.jacbts.2022.06.004
32. Zhou H, Zhang Q, Huang W, He C, Zhou C, Zhou J, et al. Epigenetic silencing of ZCCHC10 by the lncRNA SNHG1 promotes progression and venetoclax resistance of acute myeloid leukemia. Int J Oncol. 2023;62(5):64. doi:10.3892/ijo.2023.5512
33. Li H, Tian X, Wang P, Hu J, Qin R, Xu R, et al. LINC01128 resisted acute myeloid leukemia through regulating miR-4260/NR3C2. Cancer Biol Ther. 2020;21(7):615–22. doi:10.1080/15384047.2020.1740054
34. Wang K, Reichermeier KM, Liu X. Quantitative analyses for effects of neddylation on CRL2(VHL) substrate ubiquitination and degradation. Protein Sci. 2021;30(11):2338–45. doi:10.1002/pro.4176
35. Zhou W, Xu J, Tan M, Li H, Li H, Wei W, et al. UBE2M is a stress-inducible dual E2 for neddylation and ubiquitylation that promotes targeted degradation of UBE2F. Mol Cell. 2018;70(6):1008–24.e6. doi:10.1016/j.molcel.2018.06.002